Available online at www.sciencedirect.com
SCIENCE DIRECT®
Thermochimica Acta 408 (2003) 1–7
thermochimica acta
www.elsevier.com/locate/tca

Enthalpy of mixing in liquid Al–Fe–Si alloys at 1750 K

D.S. Kanibolotsky [a,b,*], O.A. Bieloborodova [a], N.V. Kotova [a], V.V. Lisnyak [a,*]

[a] *Department of Inorganic Chemistry, Chemical Faculty, Kyiv National Taras Shevchenko University, Volodymyrska Str. 64, 01033 Kyiv, Ukraine*
[b] *Biophysical Department, Academician Bogach Institute for Physiology, Glushkova Ave. 2, Corp. 12, 03022 Kyiv, Ukraine*

Received 11 December 2002; received in revised form 15 May 2003; accepted 15 May 2003

Abstract

The partial for aluminium and integral enthalpies of mixing in liquid Al–Fe–Si alloys have been measured by high-temperature isoperibolic calorimetry at 1750 ± 5 K. The study has been performed along five sections with constant concentration ratios of Si and Fe. The integral enthalpies of mixing were simulated according Bonnier geometry. The differences between experimental and simulated data possess negative values within the experimental errors range, which may testify that ternary interaction is negligibly small at the experimental temperature.

Keywords: Al–Fe–Si; Liquid alloys; Calorimetry; Enthalpy of mixing

1. Introduction

Ternary Al–Fe–Si alloys are of great interest due to commercial importance of the Fe-rich magnetic alloys (SENDUST, ALSIFER) and wide application of the Al-rich alloys in production of light constructional materials. Besides, liquid Al–Fe–Si alloys at fast quenching are capable to form amorphous phases, which properties are intensively studied last decade [1–3]. The knowledge on thermodynamic properties of the system, including a liquid state, is necessary for design and improvement of industrial alloys.

Earlier, the liquid Al–Fe–Si alloys thermodynamics have been examined using electromotive force method at temperatures: 850–1300 K [4], 1023–1373 K [5] and 873–1223 K [6] for Al-enriched field ($x_{\mathrm{Al}} \geq 0.5$). However, enthalpies of formation have been measured only for ternary solid phases by calorimetry [7–9]. Besides, the phase equilibrium study in the system is still in progress [10], therefore thermodynamics of the liquid state is required for Al–Fe–Si phase diagram assessment. Considering that Al–Fe–Si alloys are of a high-actuality, the present paper is devoted to calorimetric investigation of Al–Fe–Si melts at 1750 ± 5 K for aluminium concentrations being in the range $0 \leq x_{\mathrm{Al}} \leq 0.6$.

2. Experimental

2.1. Measuring technique and data treatment

The enthalpies of mixing were studied using a high-temperature isoperibolic calorimeter [11]. The measurements were performed under pure argon at atmospheric pressure. The experimental enthalpies

---

[*] Corresponding authors. Tel.: +380-44-2662139 (D.S. Kanibolotsky)/+380-44-4408795 (V.V. Lisnyak); fax: +380-44-2520827 (D.S. Kanibolotsky)/+380-44-2302505 (V.V. Lisnyak).
E-mail addresses: kanibolotsky@univ.kiev.ua (D.S. Kanibolotsky), lisnyak@chem.univ.kiev.ua (V.V. Lisnyak).

doi:10.1016/S0040-6031(03)00314-9

of mixing were measured by dropping of the pure solid components stated at 298 K into a liquid bath (1750 ± 5 K). Silicon bars (Alfa, 99.9999%), iron wire (Aldrich, 99.99%), aluminium wire (Alfa, 99.99%) and tungsten wire (Alfa, 99.96%) were used for calorimetric experiments. Temperature measurements were carried out using thermocouples (WRe5–WRe20). One thermocouple is situated in calorimeter core for temperature controlling. Twenty thermocouples are included in the thermopile for precision measurement of difference in the temperature between crucible with alloy and the isothermal core of calorimeter.

The initial component in the crucible was silicon (1–2.6 g). Dropping of the silicon samples into the molten silicon performed the first calorimeter calibration. After that iron was added into the melt for initial binary Fe_xSi_{1-x} alloy formation. The temperature–time curve was recorded during aluminium samples dropping into the liquid bath. The tungsten was used for the finally calorimeter calibration. The absence of interaction between tungsten and liquid alloy was controlled by mass analysis after alloy quenching and ingots cutting. The masses of dropped samples varied in the range of 0.02–0.32, 0.05–0.43, 0.02–0.32 and 0.11–0.66 g for silicon, iron, aluminium and tungsten, correspondingly. The samples masses were measured with the maximal deviation 10^{-4} g. The elements enthalpies of heating were taken from [12].

The measurements were performed at 1750 ± 5 K along five sections with constant x_{Si}:x_{Fe} ratio of 0.3:0.7, 0.4:0.6, 0.5:0.5, 0.7:0.3 and 0.85:0.15 for $0.0 \leq x_{Al} \leq 0.6$. Partial enthalpy of mixing was calculated by following expression:

$$\Delta_{mix}\bar{H}_{Al} = -\Delta H^{T}_{298} + \frac{k}{n_{Al}}\int_{0}^{\tau_\infty}\Delta T\,dt, \qquad (1)$$

where ΔH^{T}_{298} is the molar enthalpy of aluminium heating from 298 K up to experimental temperature, k is the thermal coefficient of calorimeter, n_{Al} is the quantity of dropped sample (mol), t and τ_∞ are the total experimental time and the time of temperature relaxation and ΔT is the difference between temperature of melt at the moment t and equilibrium temperature of the melt after relaxation.

Experimental aluminium partial enthalpies of mixing were presented via α_{Al}-function ($\alpha_{Al} = \Delta_{mix}\bar{H}_{Al}/(1-x_{Al})^2$). The α_{Al}-function was smoothed using least square regression (l.s.r.) for polynomial equation of form:

$$\alpha_{Al} = Q_0 + Q_1x_{Al} + Q_2x_{Al}^2 + \cdots + Q_jx_{Al}^j, \qquad (2)$$

where Q_j are the polynomial coefficients, x_{Al} is the aluminium mole fraction and j is the polynomial degree determined by the Fisher's exact test. Integral enthalpy of mixing was calculated in accordance with Darken's method:

$$\Delta_{mix}H = (1-x_{Al})\left[\int_0^{x_{Al}}\alpha_{Al}\,dx_{Al} + \Delta_{mix}H^\circ\right], \qquad (3)$$

where $\Delta_{mix}H^\circ$ is the integral enthalpy of mixing in binary Fe–Si alloys [11].

After substitution of Eq. (2) in Eq. (3) and integration, the Eq. (3) should be as follows:

$$\Delta_{mix}H = (1-x_i)\left(\Delta_{mix}H^\circ + Q_0x_{Al} + \frac{1}{2}Q_1x_{Al}^2 + \cdots + \frac{1}{j+1}Q_jx_{Al}^{j+1}\right). \qquad (4)$$

The integral enthalpies of mixing deviations were determined as discussed below. In accordance with probability theory the dispersion of complicated function $f(\varphi_1, \varphi_2, \varphi_3, \ldots, \varphi_n)$ should be given by the following equation:

$$D(f(\varphi_1, \varphi_2, \varphi_3, \ldots, \varphi_n)) = \sum_{i=1}^{n}\left(\frac{d f(\varphi_i)}{d\varphi_i}\right)^2 D(\varphi_i), \qquad (5)$$

where $D(\varphi_i)$ is the dispersion of φ_i. According to Eq. (3), the integral enthalpy of mixing is a complicated function of $\Delta_{mix}H^\circ$ and α_{Al}. Therefore, the dispersion of mixing enthalpy ($D(\Delta_{mix}H)$) can be presented as a sum of D_1 and D_2. This approach leads to

$$D(\Delta_{mix}H) = D_1 + D_2 = \left(\frac{d\Delta_{mix}H}{d\Delta_{mix}H^\circ}\right)^2 D(\Delta_{mix}H^\circ) + \left(\frac{d\Delta_{mix}H}{d\alpha_{Al}}\right)^2 D(\alpha_{Al}). \qquad (6)$$

The part of integral enthalpy dispersion, which depends on dispersion of integral enthalpy of mixing in the boundary system, can be defined by

$$D_1 = (1-x_{Al})^2 D(\Delta_{mix}H^\circ). \qquad (7)$$

Hereafter we consider the part of integral enthalpy dispersion, depending on α_{Al}-function dispersion, i.e. D_2. The integral in Eq. (3) can be described as a sum:

$$(1-x_{\mathrm{Al}})\int_0^{x_{\mathrm{Al}}} \alpha_{\mathrm{Al}}\,\mathrm{d}x_{\mathrm{Al}} = (1-x_{\mathrm{Al}})\sum_0^{x_i} \alpha_{\mathrm{Al}}\Delta x_{\mathrm{Al}}. \quad (8)$$

Consequently, the D_2 part of $D(\Delta_{\mathrm{mix}}H)$ is equal to following expression:

$$\begin{aligned} D_2 &= (1-x_{\mathrm{Al}})^2 \sum_0^{x_{\mathrm{Al}}} D(\alpha_{\mathrm{Al}})(\Delta x_{\mathrm{Al}})^2 \\ &= (1-x_{\mathrm{Al}})^2 \int_0^{x_{\mathrm{Al}}} D(\alpha_{\mathrm{Al}})(\Delta x_{\mathrm{Al}})\,\mathrm{d}x_{\mathrm{Al}}. \end{aligned} \quad (9)$$

The variable Δx_{Al} is indefinite, thus Eq. (9) contains the indefinite integral. For this reason in initial approximation α_{Al} and $D(\alpha_{\mathrm{Al}})$ can be considered as practically independent from i-component concentration. So, the second part of integral enthalpy dispersion should be as

$$\begin{aligned} D_2 &= (1-x_{\mathrm{Al}})^2 \left(\frac{\mathrm{d}}{\mathrm{d}\alpha_{\mathrm{Al}}}\int_0^{x_{\mathrm{Al}}} \alpha_{\mathrm{Al}}\,\mathrm{d}x_{\mathrm{Al}}\right)^2 D(\alpha_{\mathrm{Al}}) \\ &= x_{\mathrm{Al}}^2(1-x_{\mathrm{Al}})^2 D(\alpha_{\mathrm{Al}}). \end{aligned} \quad (10)$$

Resulted dispersion $D(\Delta_{\mathrm{mix}}H)$ after substitution of Eqs. (7) and (10) in Eq. (6) should be given as

$$\begin{aligned} D(\Delta_{\mathrm{mix}}H) &= (1-x_{\mathrm{Al}})^2 (D(\Delta_{\mathrm{mix}}H^{\circ}) \\ &\quad + x_{\mathrm{Al}}^2 D(\alpha_{\mathrm{Al}})). \end{aligned} \quad (11)$$

Thus, as dispersion $D(\alpha_{\mathrm{Al}})$ nevertheless is a function of x_{Al}, the average dispersion of alpha function on a range from 0 to x_i should be substituted in Eq. (11):

$$\begin{aligned} &D(\Delta_{\mathrm{mix}}H) \\ &= (1-x_{\mathrm{Al}})^2 \left(D(\Delta_{\mathrm{mix}}H^{\circ}) + x_{\mathrm{Al}}^2 \frac{\int_0^{x_{\mathrm{Al}}} D(\alpha_{\mathrm{Al}})\,\mathrm{d}x_{\mathrm{Al}}}{x_{\mathrm{Al}}}\right) \\ &= (1-x_{\mathrm{Al}})^2 \left(D(\Delta_{\mathrm{mix}}H^{\circ}) + x_{\mathrm{Al}} \int_0^{x_{\mathrm{Al}}} D(\alpha_{\mathrm{Al}})\,\mathrm{d}x_{\mathrm{Al}}\right). \end{aligned} \quad (12)$$

Consequently, root-mean-square deviation of integral enthalpy of mixing is

$$\begin{aligned} \sigma(\Delta_{\mathrm{mix}}H) &= (1-x_{\mathrm{Al}}) \\ &\quad \times \sqrt{D(\Delta_{\mathrm{mix}}H^{\circ}) + x_{\mathrm{Al}} \int_0^{x_{\mathrm{Al}}} D(\alpha_{\mathrm{Al}})\,\mathrm{d}x_{\mathrm{Al}}}. \end{aligned} \quad (13)$$

The confidence interval of enthalpies of mixing was calculated using the Student's coefficient for 95% probability, which is equal to 2.

2.2. Interpolation of the integral enthalpy of mixing for ternary alloys

The interpolation method proposed in [13] was used for presentation of ternary alloys thermodynamics. Corresponding to the method, the simulation of integral enthalpies of mixing in ternary system is performed by one of geometric models. The difference between experimental data for sections and calculated via geometric model is treated by l.s.r.

For studied Al–Fe–Si system the Bonier geometric model [14] is optimal algorithm because liquid alloys of one boundary binary system relate to regular solution (Al–Si [15]), whereas in two others (Al–Fe [16] and Fe–Si [11]) the strong component interaction is observed. Integral enthalpies of mixing for the boundary Fe–Si [11], Al–Si [15] systems and optimised data set of [17] for Al–Fe system were used for the simulation.

3. Results and discussion

Experimentally determined partial mixing enthalpies of aluminium along sections with constant $x_{\mathrm{Si}}:x_{\mathrm{Fe}}$ ratio are plotted on Fig. 1. The Q_j coefficients for the α_{Al}-function (Eq. (2)) are listed in Table 1 (in kJ mol^{-1}).

The interpolation method adequately describes the experimental results in whole studied composition range by the equation

Table 1
Evaluated Q_j coefficients for Eq. (2), which approximates the α_{Al}-function for Al–Fe–Si radial sections

j	$x_{\mathrm{Si}}:x_{\mathrm{Fe}}$				
	0.3:0.7	0.4:0.6	0.5:0.5	0.7:0.3	0.85:0.15
0	−26.8	−22.2	−252.0	−24.0	−20.5
1	−99.4	7.5	76.9	85.6	99.8
2	163.8	−65.8	−54.7	−167.4	−627.9
3	0	0	0	0	927.3

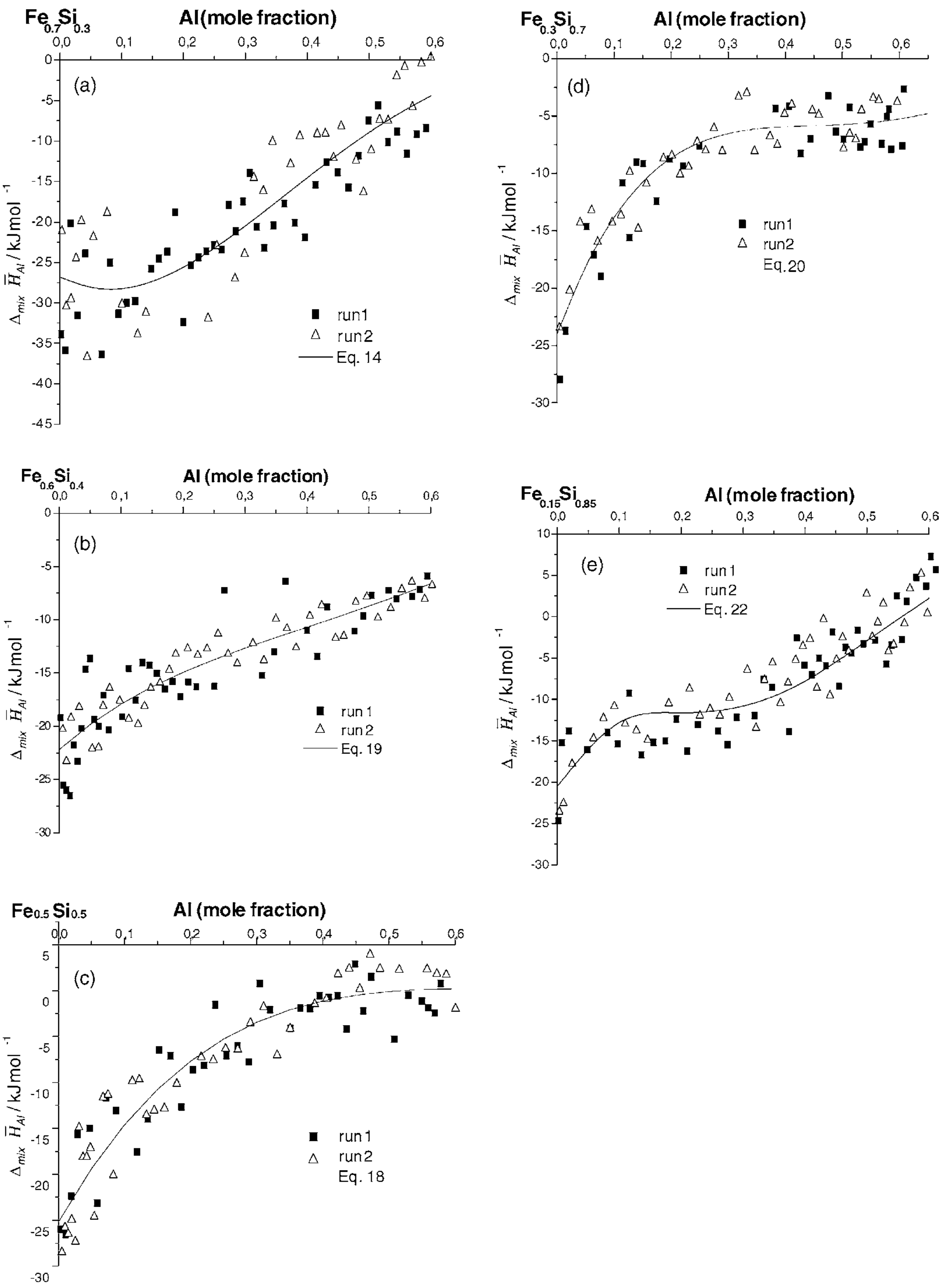

Fig. 1. Partial enthalpy of mixing of aluminium for studied sections (a–e) of liquid Al–Fe–Si alloys at 1750 ± 5 K.

$$\begin{aligned}\Delta_{\text{mix}}H = {} & \frac{x_{\text{Al}}}{x_{\text{Al}}+x_{\text{Si}}}\Delta_{\text{mix}}H_{\text{Al–Fe}}(x_{\text{Fe}}) \\ & + \frac{x_{\text{Si}}}{x_{\text{Al}}+x_{\text{Si}}}\Delta_{\text{mix}}H_{\text{Fe–Si}}(x_{\text{Fe}}) \\ & + (x_{\text{Al}}+x_{\text{Si}})\Delta_{\text{mix}}H_{\text{Al–Si}}\left(\frac{x_{\text{Al}}}{x_{\text{Al}}+x_{\text{Si}}}\right) \\ & + \Delta_{\text{mix}}H_{\text{Al–Fe–Si}}, \qquad (14)\end{aligned}$$

where integral enthalpy of mixing in boundary binary alloys are represented by following relationships (in kJ mol^{-1}):

$$\begin{aligned}\Delta_{\text{mix}}H_{\text{Al–Fe}} = {} & x_{\text{Fe}}(1-x_{\text{Fe}})(-63.15-60.86(1-x_{\text{Fe}}) \\ & + 114.62(1-x_{\text{Fe}})^2-193.85(1-x_{\text{Fe}})^3 \\ & + 108.94(1-x_{\text{Fe}})^4), \qquad (15)\end{aligned}$$

$$\begin{aligned}\Delta_{\text{mix}}H_{\text{Fe–Si}} = {} & x_{\text{Fe}}(1-x_{\text{Fe}})(-99.44-60.46x_{\text{Fe}} \\ & - 177.15x_{\text{Fe}}^2 + 191.06x_{\text{Fe}}^3), \qquad (16)\end{aligned}$$

$$\begin{aligned}& \Delta_{\text{mix}}H_{\text{Al–Si}} \\ & = \frac{x_{\text{Al}}}{x_{\text{Al}}+x_{\text{Si}}}\left(1-\frac{x_{\text{Al}}}{x_{\text{Al}}+x_{\text{Si}}}\right) \\ & \times\left[-2.85-72.01\frac{x_{\text{Al}}}{x_{\text{Al}}+x_{\text{Si}}}+78.17\left(\frac{x_{\text{Al}}}{x_{\text{Al}}+x_{\text{Si}}}\right)^2\right]. \qquad (17)\end{aligned}$$

The contribution of fourth term of Eq. (14), which may be partially attributed to ternary interactions, derived by the formula (in kJ mol^{-1}):

$$\begin{aligned}& \Delta_{\text{mix}}H_{\text{Al–Fe–Si}} \\ & = x_{\text{Al}}x_{\text{Si}}(1-x_{\text{Al}}-x_{\text{Si}})(20.84-345.5x_{\text{Al}} \\ & - 152.9x_{\text{Si}} + 125.3x_{\text{Al}}^2 - 55.2x_{\text{Si}}^2 \\ & + 920.6x_{\text{Si}}x_{\text{Al}}). \qquad (18)\end{aligned}$$

As it can be seen from Fig. 2a, the Bonier geometry corresponds well to experimental data; the differences between experimental and simulated data (Eq. (18)) are insignificant negative values. The maximal difference between experimental and calculated $\Delta_{\text{mix}}H$ is -1.5 kJ mol^{-1} at $0.1 < x_{\text{Si}} < 0.3$ and $0.3 < x_{\text{Al}} < 0.7$ (Fig. 2b), that is no more than experimental error. Because of this, thermodynamics of ternary Al–Fe–Si alloys at 1750 K is preferably characterised by interaction between components in the boundary binary systems.

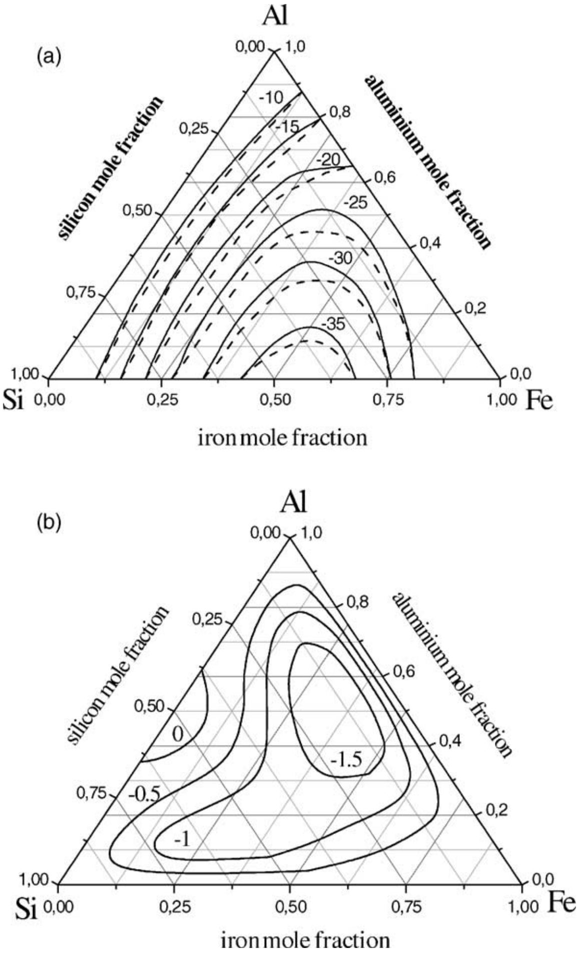

Fig. 2. (a) Projection of isoenthalpic lines on the Gibbs–Roseboom triangle; solid lines are experimental data, dashed lines are data calculated by Bonier model. (b) The contribution of the term $\Delta_{\text{mix}}H_{\text{Al–Fe–Si}}$ in Eq. (14) (in kJ mol^{-1}).

As one can see from Table 2, liquid Al–Fe–Si alloys are formed with significant calorification. The integral enthalpies of mixing reach the extreme for ternary alloys composition close to Fe–Si boundary system. This fact can be explained adequately by presence of refractory iron monosilicide ($T_{\text{m}} = 1683 \pm 3$ K) in solid Fe–Si alloys [18]. The strong intercomponent interaction is remained in the melt at insignificant overheating above liquidus curve. It promotes formation of clusters with composition nearby to FeSi stoichiometry [19]. The binary Fe–Si clusters can exist also in the ternary alloys, according to the concentration depen-

Table 2
The enthalpies of mixing in liquid Al–Fe–Si alloys

x_{Al}	x_{Si}:x_{Fe}				
	0.3:0.7	0.4:0.6	0.5:0.5	0.7:0.3	0.85:0.15
$\Delta\bar{H}_{Al} \pm 2\sigma$ (kJ mol^{-1})					
0.0	−26.8 ± 6.6	−22.2 ± 3.1	−25.2 ± 3.5	−24.0 ± 4.2	−20.5 ± 11.2
0.1	−28.4 ± 3.0	−17.9 ± 1.5	−14.6 ± 1.6	−13.8 ± 1.8	−12.8 ± 5.0
0.2	−25.7 ± 2.4	−14.9 ± 1.4	−7.7 ± 1.4	−8.7 ± 1.4	−11.6 ± 3.4
0.3	−20.5 ± 2.0	−12.7 ± 1.3	−3.5 ± 1.2	−6.5 ± 1.2	−10.8 ± 2.2
0.4	−14.5 ± 1.3	−10.7 ± 0.8	−1.2 ± 0.8	−5.9 ± 0.8	−7.8 ± 1.1
0.5	−8.9 ± 1.0	−8.7 ± 0.6	−0.1 ± 0.6	−5.7 ± 0.5	−2.9 ± 1.1
0.6	−4.4 ± 1.2	−6.6 ± 0.7	0.2 ± 0.7	−5.3 ± 0.6	2.2 ± 1.5
$\Delta_{mix}H \pm 2\sigma$ (kJ mol^{-1})					
0.0	−34.2 ± 2.3	−38.0 ± 2.7	−37.5 ± 1.3	−27.0 ± 1.0	−14.3 ± 0.7
0.1	−33.6 ± 2.1	−36.2 ± 2.5	−35.7 ± 1.2	−26.1 ± 0.9	−14.4 ± 1.0
0.2	−32.9 ± 2.0	−34.0 ± 2.2	−32.9 ± 1.1	−24.4 ± 0.9	−14.2 ± 1.4
0.3	−31.7 ± 1.9	−31.4 ± 2.0	−29.5 ± 1.0	−22.3 ± 0.9	−13.9 ± 1.0
0.4	−29.6 ± 1.8	−28.6 ± 1.7	−25.6 ± 1.0	−20.0 ± 0.9	−13.2 ± 1.7
0.5	−26.6 ± 1.6	−25.4 ± 1.5	−21.4 ± 0.9	−17.6 ± 0.8	−11.9 ± 1.6
0.6	−22.6 ± 1.5	−21.9 ± 1.3	−17.1 ± 0.8	−15.2 ± 0.7	−9.5 ± 1.7

dence of integral enthalpy of mixing (Fig. 2a). This conclusion is in agreement with Al–Fe–Si phase diagram, which contains wide field of the iron monosilicide primary crystallisation [10,20].

Aluminium with silicon interacts more weakly than aluminium with iron [15,17]. Therefore, it may be suggested logically, that the aluminium partial enthalpies of mixing would be more negative in the case of x_{Si}:x_{Fe} ratio decreasing. However, their absolute values became less and reach minimum for x_{Si}:x_{Fe} = 0.5:0.5 section in the contradiction to our assumption. The similar phenomenon also was observed earlier in [6] for thermodynamic activity of aluminium. The minimal negative deviations from Raoultian for aluminium is characteristic for the same section of ternary system (x_{Si}:x_{Fe} = 0.5:0.5).

All this can be obviously a consequence of the suppression of weak interaction between aluminium and silicon by stronger one of iron and silicon. On the other hand, interaction between aluminium and iron at decreasing of x_{Si}:x_{Fe} ratio from 0.5:0.5–0 is resulted in increasing of both $\Delta_{mix}\bar{H}_{Al}$ absolute values (see Fig. 1) and negative deviation from Raoultian [6]. Consequently, the contribution of component interaction in boundary Fe–Si system determines the ternary alloys thermodynamics. Moreover, comparison of literature data [7–9] on formation enthalpy for ternary intermetallides with mixing enthalpies calculated by Eq. (14) was performed for estimation of possible ternary interaction. It is known, that in the case of essential ternary interaction in the system these values must be in agreement. As one can see from Table 3, intermetallics form with more significant calorification than appropriate melts. This can be complementary evidence conforming absence of strong ternary interaction at 1750 K in studied melts.

Table 3
Solid ternary phases formation enthalpy and mixing enthalpy of liquid alloys

Ternary alloys composition	$\Delta_f H$ (kJ mol^{-1})	$\Delta_{mix}H$ (kJ mol^{-1})
$Al_{0.36}Fe_{0.36}Si_{0.28}$	−36.7 ± 1.9 [8]	−29.4
$Al_{0.38}Fe_{0.32}Si_{0.3}$	−35.8 ± 1.8 [9]	−27.9
$Al_{0.4}Fe_{0.4}Si_{0.2}$	−34.2 ± 1.6 [8]	−28.9
$Al_{0.42}Fe_{0.39}Si_{0.19}$	−35.7 ± 1.4 [8]	−28.3
$Al_{0.48}Fe_{0.15}Si_{0.37}$	−19.2 ± 1.3 [9]	−17.3
$Al_{0.5}Fe_{0.25}Si_{0.25}$	−29.6 ± 0.9 [9]	−23.3
$Al_{0.538}Fe_{0.154}Si_{0.308}$	−20.5 ± 1.2 [9]	−17.2
$Al_{0.58}Fe_{0.22}Si_{0.20}$	−28.4 ± 1.9 [9]	−20.6
$Al_{0.6}Fe_{0.2}Si_{0.2}$	−25.3 ± 1.6 [9]	−19.3
$Al_{0.60}Fe_{0.25}Si_{0.15}$	−30.4 ± 1.9 [8]	−21.5
$Al_{0.70}Fe_{0.15}Si_{0.15}$	−24.5 ± 2.0 [7]	−14.9
$Al_{0.70}Fe_{0.15}Si_{0.15}$	−20.2 ± 0.9 [9]	−14.9
$Al_{0.72}Fe_{0.18}Si_{0.10}$	−34.3 ± 2.0 [7]	−16.2
$Al_{0.72}Fe_{0.18}Si_{0.10}$	−24.4 ± 1.4 [8]	−16.2

4. Conclusions

It has been established that the liquid Al–Fe–Si alloys are formed with significant calorification up to $-35\,\mathrm{kJ\,mol^{-1}}$. The concentration dependencies of partial for aluminium and integral enthalpies of mixing testify that thermodynamic properties of Al–Fe–Si alloys are predominantly determined by component interaction in Fe–Si boundary system.

Acknowledgements

The authors thankful greatly the financial support of the National Ministry of Science and Education (Grant #0197U003067).

References

[1] H.S. Cho, H.G. Jeong, M.S. Kim, H. Yamagata, Scripta Mater. 42 (2000) 221.
[2] M. Calin, M. Petrescu, Sci. Bull. Chem. Mater. Sci. Polytechn. Inst. (Bucharest) 54 (1992) 151.
[3] D.V. Louzguine, A. Takeuchi, A. Inoue, Mater. Trans. JIM 38 (1997) 595.
[4] M. Bonnet, J. Rogez, R. Castanet, Thermochim. Acta 155 (1989) 39.
[5] H. Nagai, H. Mitani, J. Jpn. Inst. Met. 14 (1973) 130.
[6] J. Peracis, P. Desre, Rev. Int. H-tes. Temp. Refract. 10 (1973) 79.
[7] M. Vybornov, P. Rogl, F. Sommer, J. Alloys Compd. 247 (1997) 154.
[8] Y. Li, P. Ochin, A. Quivy, P. Telolahy, B. Legendre, J. Alloys Compd. 298 (2000) 198.
[9] Y. Li, B. Legendre, J. Alloys Compd. 302 (2000) 187.
[10] Z.-K. Liu, Y.A. Chang, Metall. Mater. Trans. A 30 (1999) 1081.
[11] D.S. Kanibolotsky, O.A. Bieloborodova, N.V. Kotova, V.V. Lisnyak, J. Therm. Anal. Cal. 71 (2003) 583.
[12] A.T. Dinsdale, CALPHAD 15 (1991) 317.
[13] V.T. Witusiewicz, I. Arpshofen, H.-J. Seifert, F. Sommer, F. Aldinger, Z. Metallknd. 91 (2000) 128.
[14] E. Bonnier, R. Caboz, Compt. Rend. Acad. Sci. (Paris) 250 (1960) 527.
[15] D.S. Kanibolotsky, E.A. Bieloborodova, N.V. Kotova, V.V. Lisnyak, J. Therm. Anal. Cal. 70 (2002) 175.
[16] N.S. Jacobson, High Temp. Mater. Sci. 35 (1996) 1.
[17] M.S. Petrushevsky, Yu.O. Yesin, P.V. Geld, V.M. Sandakov, Izv. Akad Nauk USSR Metally 6 (1972) 193.
[18] B. Massalski, Binary Alloy Phase Diagrams, vols. 1 and 2, ASM, Metals Park, OH, 1990, p. 2224.
[19] G.K. Moiseyev, N.I. Ilyinyh, N.A. Vatolin, S.I. Zaytseva, Zh. Fiz. Khimii 69 (1995) 1596.
[20] V. Raghavan, J. Phase Equilib. 15 (1994) 414.